

# Fentanyl and Its Analogue *N*-[1-(2-Phenylethyl)-4-piperidyl]-*N*-[1-(2-phenylethyl)-4-piperidyl]propanamide: <sup>1</sup>H- and <sup>13</sup>C-NMR Spectroscopy, X-Ray Crystallography, and Theoretical Calculations

María Luisa JIMENO,<sup>a</sup> Ibon ALKORTA,<sup>a</sup> Carolina CANO,<sup>a</sup> Nadine JAGEROVIC,<sup>\*a</sup> Pilar GOYA,<sup>a</sup> José ELGUERO,<sup>a</sup> and Concepción FOCES-FOCES<sup>b</sup>

<sup>a</sup>Instituto de Química Médica, Consejo Superior de Investigaciones Científicas; Juan de la Cierva, 3, E-28006 Madrid, Spain; and <sup>b</sup>Departamento de Cristalografía, Instituto de Química-Física 'Rocasolano'; Serrano, 119, E-28006 Madrid, Spain. Received February 21, 2003; accepted April 21, 2003

The oxalate salts and free bases of fentanyl and *N*-[1-(2-phenylethyl)-4-piperidyl]-*N*-[1-(2-phenylethyl)-4-piperidyl]propanamide, a new lead compound for long-acting analgesia, have been characterized by <sup>1</sup>H- and <sup>13</sup>C-NMR spectroscopy. The crystal structure of the hydrochloride of *N*-[1-(2-phenylethyl)-4-piperidyl]-*N*-[1-(2-phenylethyl)-4-piperidyl]propanamide monohydrate has been determined. Two centrosymmetrically related cations, joined through C(phenyl)-H... $\pi$  contacts, encapsulate a large void that contains pairs of anions and bridged water molecules into a zero-dimensional (0D) supramolecular motif. The cations are linked to this framework *via* N<sup>+</sup>H...Cl<sup>-</sup> contacts. GIAO/B3LYP calculations have been carried out to compare the experimental <sup>13</sup>C chemical shifts with the absolute shieldings thus calculated. The protonation of both molecules takes place on the piperidine ring (axial protonation), as has been verified both in the solid state (X-ray) and in solution (NMR).

**Key words** pyrazole; analgesia; fentanyl; crystal structure; GIAO; B3LYP

4-Anilinopiperidine derivatives have been the subject of considerable interest<sup>1,2)</sup> due to their analgesic properties. *N*-[1-(2-Phenylethyl)-4-piperidyl]-*N*-phenylpropanamide<sup>3)</sup> (fentanyl (**1**), see Fig. 1), the clinically most important member of this family, is characterized by very high potency as well as rapid onset and short duration of action. The use of fentanyl *via* transdermal administration for the treatment of oncologic and chronic pain creates the need for long-acting fentanyl derivatives.<sup>4–7)</sup> The recently published *in vivo* pharmacological studies<sup>8)</sup> of *N*-[1-(2-phenylethyl)-4-piperidyl]-*N*-(1-phenyl-4-pyrazolyl)propanamide (**2**) (see Fig. 1), a new member of the 4-anilinopiperidine family with long-acting analgesic properties confers on this compound a unique position within this group. In comparison with fentanyl and despite its potent and selective  $\mu$  opioid agonist properties (**2**,  $K_i=0.032$  nM; **1**,  $K_i=5.9$  nM), **2** was found to be a less potent analgesic in the hot plate test in mice. However, **2** showed a three-fold longer duration of analgesia in this test (**2**, 360 min; **1**, 120 min).

Structure–activity relationship (SAR) studies<sup>1,2,9–14)</sup> in the fentanyl series have led to the discovery of compounds with diverse analgesic profiles (carfentanil, alfentanil, sufentanil, lofentanil, mirfentanil, remifentanil, ohmefentanil, 4-methylfentanil, *etc.*). Among the *N*-phenylpropanamide group modifications that have been reported, only few heterocyclic (six-membered rings, pyrroles, and fused-ring types) substitutions of the phenyl ring have been described.<sup>15,16)</sup> The resulting compounds combined another structural modification: the propanamide group was substituted by a methoxyacetamide residue known to confer short duration of action, and these compounds have generally shown weaker analgesic effects than fentanyl. Within this context, the fentanyl analogue **2** has an especially interesting pharmacological profile and deserves more complete structural study.

Despite the importance of fentanyl and the fact that it has been the subject of a large number of structural and conformational studies,<sup>17–23)</sup> the basis of fentanyl binding is still

under investigation.<sup>24)</sup> According to the Cambridge Crystallographic Database (CSD)<sup>25)</sup> the crystal structure of the citrate salt of **1**<sup>26)</sup> and that of citrate-toluene solvate<sup>27)</sup> have been solved. The crystallographic data of the latter compound have been combined with interactive molecular graphics techniques on a series of fentanyl analogues to carry out a comparative conformational analysis (no atomic coordinates for the citrate salt of **1**<sup>26)</sup> are available). Using PCILO calculations, 306 possible conformations have been found for fentanyl.<sup>28)</sup> Subsequently, MM2 and semiempirical AM1 calculations<sup>23)</sup> proposed a chair conformation for the piperidine ring with an axial anilide group which agrees with <sup>1</sup>H- and <sup>13</sup>C-NMR spectroscopic data.<sup>29,30)</sup>

The crystal structures of various fentanyl derivatives have mainly been reported as part of SAR studies.<sup>25,31–38)</sup> Recently, the X-ray analysis of the ohmefentanil derivatives allowed determination of the absolute configuration of stereoisomers of this potent analgesic.<sup>39)</sup>

Our purpose is to contribute to the structural characterization of fentanyl (**1**) and its analogue *N*-[1-(2-phenylethyl)-4-

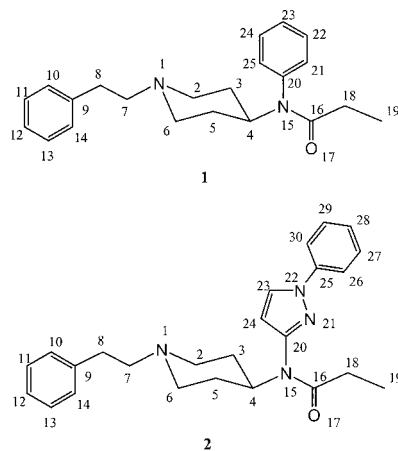


Fig. 1. Structures of Fentanyl (**1**) and Fentanyl Derivative (**2**)

\* To whom correspondence should be addressed. e-mail: nadine@iqm.csic.es

Table 1.  $^1\text{H}$ - and  $^{13}\text{C}$ -NMR Chemical Shifts (ppm) and Coupling Constants,  $J_{\text{H,H}}$  (Hz) for Fentanyl (**1**) in  $\text{CDCl}_3$  and  $^{13}\text{C}$ -NMR Chemical Shifts (ppm) of the Free Base **1** in  $\text{CF}_3\text{CO}_2\text{H}$  at  $20^\circ\text{C}^a$ 

C, H No.	Free base <b>1</b>		Oxalate <b>1H</b> <sup>+</sup>			Free base <b>1</b>	Oxalate <b>1H</b> <sup>+</sup>	<b>1H</b> <sup>+</sup>
	$\delta_{\text{C}}$	$\delta_{\text{H}}$ mult.	$\delta_{\text{C}}$	$\delta_{\text{H}}$ mult.		$J_{\text{H,H}}$	$J_{\text{H,H}}$	$\text{CF}_3\text{CO}_2\text{H}$ , $\delta_{\text{C}}$
2, 6ax	53.32	2.10 bt	52.85	2.73 bt	2ax, 2eq	11.7	12.2	52.97
eq		2.94 bd		3.58 bd	2ax, 3ax	11.5	12.2	
3, 5ax	30.73	1.37 bq	27.84	1.76 qd	3ax, 3eq	12.0	12.9	27.99
eq		1.74 bd		1.89 bd	3ax, 4	12.2	12.9	
4	52.29	4.62 tt	49.90	4.73 tt	3ax, 2eq	n.d.	3.5	49.75
7	60.72	2.47 m	58.64	3.06 m	3eq, 4	3.9	3.7	58.82
8	34.03	2.66 m	30.94	2.89 m	7, 8	n.d.	n.d.	30.87
9	140.40		136.27		18, 19	7.4	7.5	135.90
10, 14	128.87	7.08 d	128.85	7.05 d	10, 11	7.5	7.7	128.79
11, 13	128.63	7.19 dd	129.21	7.20 dd	11, 12	7.2	7.2	129.46
12	126.29	7.11 t	127.53	7.15 t	21, 22	7.5	6.7	127.86
20	139.02		137.87		22, 23	7.0	6.8	137.54
21, 25	130.67	7.01 d	129.99	6.96 d				129.94
22, 24	129.54	7.32 dd	130.10	7.35 dd				130.33
23	128.52	7.30 t	129.37	7.17 t				129.71
16	173.80		174.31					175.06
18	28.76	1.86 q	28.65	1.87 q				28.76
19	9.86	0.94 t	9.69	0.93 t				9.88
$\text{C}_2\text{O}_4$			163.21					

a) ax, axial; eq, equatorial; s, singlet; d, doublet; dd, double doublet; t, triplet; q, quadruplet; b, broad; m, multiplet; n.d., not determined.

piperidyl]-*N*-(1-phenyl-4-pyrazolyl)propanamide (**2**) combining different techniques such as  $^1\text{H}$ - and  $^{13}\text{C}$ -NMR spectroscopy, theoretical calculations, and, in the case of the monohydrate of the hydrochloride salt of **2**, X-ray crystallography.

## Results and Discussion

**$^1\text{H}$ - and  $^{13}\text{C}$ -NMR Spectroscopy** Complete assignments of  $^1\text{H}$ - and  $^{13}\text{C}$ -NMR spectra of fentanyl (**1**), both as a free base and as oxalate (**1H**<sup>+</sup>), are given in Table 1. These data complete the partial data published previously in the literature.<sup>29,30</sup> The  $^1\text{H}$ -NMR spectra, analyzed from  $^1\text{H}$ - $^1\text{H}$  shift-correlation spectroscopy (COSY) and nuclear Overhauser enhancement spectroscopy (NOESY) experiments provided definite criteria for distinguishing axial and equatorial protons of the piperidine ring. Analysis of the  $^{13}\text{C}$ -NMR spectra was facilitated by the use of heteronuclear multiple-quantum coherence (HMQC). As proposed by previous studies, our NMR data suggest that the chair conformation of the piperidine ring with the 4-anilido group in an equatorial position is the preferred form in solution. The coupling pattern of H-7 and H-8 is consistent with a piperidine nitrogen inversion. A comparative structural analysis between the base and the oxalate reveals strong similarity between the two, indicating that in solution the protonation/deprotonation process is fast in the NMR time scale. This allows the inversion process to take place.

The assignments (chemical shifts, multiplicities, and coupling constants) for protons and carbons of the oxalate salt of fentanyl derivative (**2**) are reported in Table 2. The elemental analysis of this compound (see Experimental) confirms that although **2** has two basic centers, N1 and N21, it is a monosalt,  $\text{HO}_2\text{C}-\text{CO}_2$  **2H**<sup>+</sup>.  $^1\text{H}$ -NMR evidence, coupled with the  $^{13}\text{C}$ -NMR data and results of 2D-NMR experiments (COSY, NOESY, HMQC) clearly indicate a chair piperidine conformation with the propanamide group in an equatorial position.

Table 2.  $^1\text{H}$ - and  $^{13}\text{C}$ -NMR Chemical Shifts (ppm), and Coupling Constants,  $J_{\text{H,H}}$  (Hz) for Fentanyl Derivative (**2**) in  $\text{CDCl}_3$  at  $20^\circ\text{C}^a$ 

C, H No.	Oxalate <b>2</b>			
	$\delta_{\text{C}}$	$\delta_{\text{H}}$ mult.	H, H	$J_{\text{H,H}}$
2, 6ax	52.97	2.76 bs	7, 8	n.d.
eq		3.65 bs	18, 19	7.5
3, 5	27.61	1.98 bm	10, 11	7.0
4	49.41	4.71 m	11, 12	7.2
7	58.75	3.11 m	26, 27	7.7
8	30.77	2.92 m	27, 28	7.4
9	136.07		23, 24	2.3
10, 14	128.86	7.07 d		
11, 13	129.24	7.21 dd		
12	127.50	7.16 t		
20	148.53			
24	106.69	6.18 d		
23	129.14	7.87 d		
25	139.77			
26, 30	119.68	7.57 d		
27, 29	129.70	7.41 dd		
28	127.58	7.26 t		
16	174.88			
18	28.26	2.12 q		
19	9.62	0.98 t		
$\text{C}_2\text{O}_4$	163.24			

a) ax, axial; eq, equatorial; s, singlet; d, doublet; dd, double doublet; t, triplet; q, quadruplet; b, broad; m, multiplet; n.d., not determined; bs, broad signal.

This conformation corresponds to that of fentanyl in solution.

Computer simulations provided further support for our assignments (see below). We have carried out GIAO/B3LYP/6-31G\* calculations<sup>41,42</sup> on the bases **1** and **2** and their cations **1H**<sup>+</sup> and **2H**<sup>+</sup>, using the X-ray structures as starting geometries for the optimization. As shown by the structures, the protonation takes place on N1 and the proton occupies an axial position (the phenethyl chain, C7–C8–Ph taking the

equatorial orientation). It is possible to compare the effect produced by the protonation (neutral fentanyl in  $\text{CDCl}_3$  and in  $\text{CF}_3\text{CO}_2\text{H}$ ) to those reported in the literature for the protonation of *N*-methylpiperidine:<sup>45)</sup>

**Crystal Structure of Monohydrate Hydrochloride Salt of 2 ( $2\text{H}^+ \text{Cl}^- \text{H}_2\text{O}$ )** The asymmetric unit of the hydrochloride salt of **2** includes a water molecule, which plays an important role in the crystal packing. The cation presents a similar pattern of bond distances and angles (Table 3) to that of the parent compound retrieved from the CSD<sup>25)</sup> (CSD refcode: PEPCIT10<sup>27)</sup>) and only differs slightly in the conformation of the common phenyl ring (Figs. 2a, 3a). Both substituents of the piperidine ring are arranged in equatorial positions, whereas the protonation occurs at the axial position on N of this ring.

The crystal structure is characterized by macrorings formed by two centrosymmetric cations [of approximate dimensions:  $\text{N15}\cdots\text{C}(9-14; x, y, z)=9.469$  and  $\text{N15}\cdots\text{C}(9-14; 1-x, -y, -z)=10.881(2) \text{ \AA}$ ] interconnected *via* edge-to-face H-bonds between the two phenyl groups (Fig. 2). The large pore of the resulting ring accommodates pairs of anions bridged by water molecules (Ow) in a  $\text{R}_4^2(8)$  dimer.<sup>46,47)</sup> Both associations are held together by means of hydrogen bonds, through a strong bond from the axial N-H of the piperidine to the Cl anion and by weak  $\text{C-H}\cdots\text{Cl}/\text{Ow}$  interactions

$1\text{H}^+$  ( $\Delta\delta$  TFA, effects > 0.20 ppm)

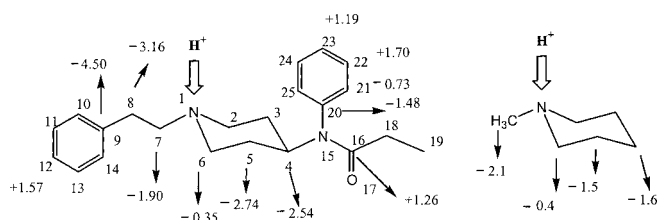


Chart 1

(Table 3, Fig. 2). The structure, as a whole, can be described as a system of layers (2D) perpendicular to *a* formed by strands (1D) along *c* (*via*  $\text{C-H}\cdots\pi$ ) and  $\text{C-H}\cdots\text{O}=\text{C}$  bonds) and connected along *b* by means of  $\text{C-H}\cdots\text{Ow}$  contacts (Fig. 4). Hence Ow and Cl anions are overall a double and quadruple acceptor of hydrogen bonds. The glide of one macroring

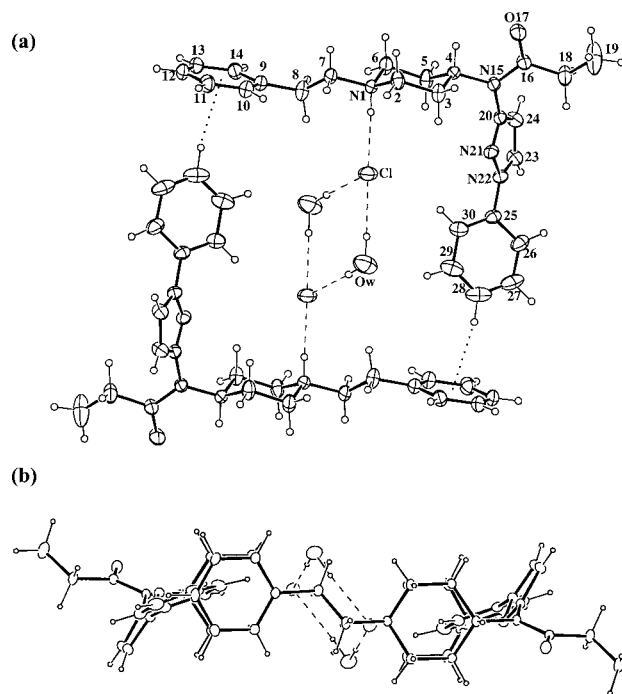


Fig. 2. (a) Supramolecular (0D) Aggregate of the Monohydrate Hydrochloride of **2** Showing the Atomic Numbering

Displacement ellipsoids are at 30% probability level, dashed lines represent hydrogen bonds.

(b) A Perpendicular View Illustrating the Disposition of the Anion and the Water Molecules in the Pore

Table 3. Selected Intra- and Intermolecular Parameters ( $\text{\AA}$ ,  $^\circ$ ). C(9—14) and C(20—25) Represent the Centroids of the C9, ..,C14 and C20, ..,C25 Phenyl Rings

O17—C16	1.221 (3)	N1—C2	1.497 (4)		
N1—C6	1.496 (3)	N1—C7	1.506 (3)		
C4—N15	1.474 (3)	C16—N15	1.363 (3)		
C20—N15	1.421 (3)	Cl $\cdots$ Cl(1-x, -y, -z)	4.992 (1)		
C2—N1—C6	110.4 (2)	C2—N1—C7	111.1 (2)		
C6—N1—C7	113.1 (2)	C4—N15—C16	119.1 (2)		
C16—N15—C20	121.7 (2)	C4—N15—C20	119.2 (2)		
N21—N22—C23	112.0 (2)	Cl $\cdots$ O1w $\cdots$ Cl(1-x, -y-z)	100.4 (1)		
N22—N21—C20	103.9 (2)	O1w $\cdots$ Cl $\cdots$ O1w(1-x, -y-z)	79.6 (1)		
C7—C8—C9—C10	-44.0 (3)	C9—C8—C7—N1	176.0 (2)		
C8—C7—N1—C2	-165.9 (2)	C3—C4—N15—C16	-94.5 (3)		
C8—C7—N1—C6	69.3 (3)	C3—C4—N15—C20	85.1 (3)		
C4—N15—C20—N21	-66.5 (3)	N21—N22—C25—C30	41.0 (3)		
C4—N15—C16—C18	176.1 (2)	N15—C16—C18—C19	-160.7 (2)		
O17—C16—N15—C20	176.4 (2)				
Hydrogen interactions		D—H	H $\cdots$ A	D $\cdots$ A	D—H $\cdots$ A
N1—H1 $\cdots$ Cl		0.99 (3)	2.14 (3)	3.041 (2)	176 (3)
Ow—H1w $\cdots$ Cl		1.00 (4)	2.24 (4)	3.241 (2)	178 (5)
Ow—H2w $\cdots$ Cl(1-x, -y, -z)		0.99 (8)	2.25 (8)	3.242 (4)	176 (6)
C29—H29 $\cdots$ O1w		0.96 (4)	2.55 (5)	3.436 (5)	153 (4)
C28—H28 $\cdots$ C(9—14)(1-x, -y, -z)		0.97 (4)	2.61 (5)	3.538 (3)	159 (5)
C3—H3b $\cdots$ C(20—25)(x, y, 1+z)		0.97 (4)	2.83 (4)	3.797 (4)	170 (3)
C8—H8b $\cdots$ O1w(x, 1+y, 1+z)		1.04 (4)	2.52 (3)	3.412 (4)	143 (3)
C23—H23 $\cdots$ O17(x, y, -1+z)		0.95 (4)	2.29 (4)	3.199 (4)	159 (2)

with respect to the neighboring ones does not allow the formation of channels, and hence pairs of anions bridged by water are encapsulated in cavities which are quite near at  $c/2$ . The layers are joined by van der Waals interactions. This packing arrangement appears to correspond to a rather close packing without voids and with a packing coefficient of 0.701.

The bond distances and angles in the  $R_4^2(8)$  dimer and the  $N^+ \cdots Cl^-$  distance is in good agreement with the averaged reported values<sup>48–50</sup> for organic structures. However, it is noteworthy that the  $N^+ \cdots Cl^-$  lengths are significantly shorter than the reported average value<sup>50</sup> for the  $(CCC)N^+ \cdots Cl^-$  and the  $Cl^- \cdots Cl^-$  distance of 4.992(1) Å is at the lowest end of the interchloride distance range for  $Cl^-$  ions bridged by a water molecule.<sup>48</sup>

The crystal structure of the citrate-toluene solvate of **1** (CSD refcode: PEPCIT10)<sup>27</sup> presents a different hydrogen bond pattern (Fig. 3). The supramolecular structure consists of a continuous 1D framework built only from anions related by a two-fold screw axis. Each cation is linked to this framework by means of a hydrogen bond from the piperidine NH

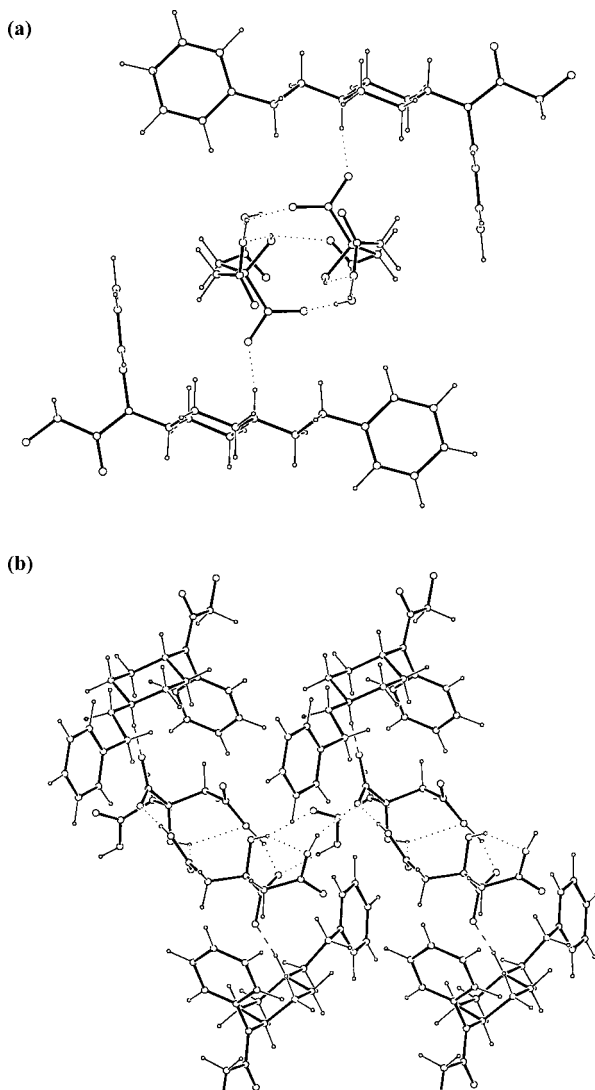


Fig. 3. Citrate Toluene Solvate of **1** (CSD Refcode: PEPCIT10)

(a) Chain of the anions, related by two-fold axis, and linked by O-H...O hydrogen bonds (dotted lines) to which the cations are bonded via  $N^+H \cdots O^-$  hydrogen interactions (dashed lines). (b) A view of the chain as projected down the  $b$  axis.

to one O of the carboxylate group. The unit cell accommodates two centrosymmetrical chains. No atomic coordinates for the citrate of **1** (CSD refcode: FENCIT)<sup>26</sup> are available.

**Theoretical Calculations: Geometry and NMR Spectroscopy** The geometries of fentanyl **1** and its cation  $1H^+$  are very close to the X-ray geometries and very similar between each other: the axial protonation of N1 has little influence on the remaining molecular parameters (distances, bond angles, and torsion angles). The same applies to the calculated and experimental geometries of cation  $2H^+$ .

We have calculated, at the GIAO/B3LYP/6-31G\* level, the absolute shieldings,  $\sigma$  in ppm, of all atoms of **1**,  $1H^+$  and  $2H^+$ . For the  $^{13}C$ -NMR data, these  $\sigma$  values have been transformed into  $\delta$  values by relationship  $\delta$  (ppm) =  $189.69 \text{ ppm} - \sigma$  (ppm), where 189.69 ppm is the value of  $\sigma(\text{TMS})$  at the same level [ $\delta(\text{TMS})=0$  by definition].

The correlation between experimental and calculated chemical shifts is excellent (the same equation holds for the values of  $1H^+$  determined using the oxalate in  $CDCl_3$  or the free base in  $CF_3CO_2H$ ):

$$\delta^{13}C_{\text{exp.}} = -(4.3 \pm 0.9) + (1.087 \pm 0.008) \delta^{13}C_{\text{calc.}}, n=51, r^2=0.997 \quad (1)$$

This confirms that the structures in solution are the same as those calculated, these last ones being almost identical to those determined by X-ray crystallography. The correlation covers a range from the methyl groups at about 10 ppm to the carbonyl ones near 175 ppm and that is partly responsible for the good fit. If one looks at the protonation effects in the case of fentanyl ( $\Delta\delta = \delta 1H^+ - \delta 1$ , in ppm), the agreement is less

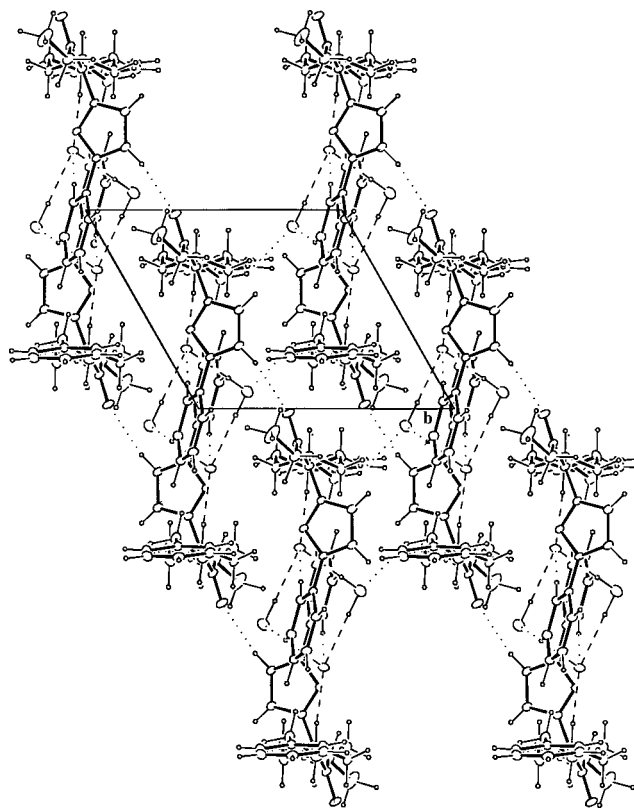


Fig. 4. Packing Diagram of the Monohydrate Hydrochloride of **2** along the  $a$  Axis Showing a Layer Formed by Two Strands (Three Macrorings on Each) Running Along the  $c$  Axis

Dotted lines represent the interactions between rings and between strands.

satisfactory:

$$\delta^{13}\text{C}_{\text{prot}}(\text{TFA}) = -(0.56 \pm 0.23) + (0.37 \pm 0.06)\delta^{13}\text{C}_{\text{prot}}(\text{calc.}),$$

$$n = 16, r^2 = 0.755 \quad (2)$$

The plot shows that four signals are clearly different (C2,6, C3,5, C7, C8). If these carbons are removed, then the correlation improves considerably:

$$\delta^{13}\text{C}_{\text{prot}}(\text{TFA}) = (0.37 \pm 0.06)\delta^{13}\text{C}_{\text{prot}}(\text{calc.}),$$

$$n = 12, r^2 = 0.977 \quad (3)$$

And for the remaining four carbons:

$$\delta^{13}\text{C}_{\text{prot}}(\text{TFA}) = -(1.98 \pm 0.05) + (0.45 \pm 0.02)\delta^{13}\text{C}_{\text{prot}}(\text{calc.}),$$

$$n = 4, r^2 = 0.995 \quad (4)$$

To put together all the signals, a dummy variable must be added (1 for C2,6, C3,5, C7, and C8 and 0 for the other 12 carbons):

$$\delta^{13}\text{C}_{\text{prot}}(\text{TFA}) = (0.38 \pm 0.02)\delta^{13}\text{C}_{\text{prot}}(\text{calc.}) - (2.00 \pm 0.13)\text{dummy},$$

$$n = 16, r^2 = 0.983 \quad (5)$$

From these equations it can be concluded: 1) GIAO calculations overestimate the experimental protonation effects (they must be multiplied by about 0.4); 2) the calculations reproduce the sign and the order of magnitude of the experimental values; and 3) the four carbons that behave differently are the  $\alpha$  and  $\beta$  carbons with regard to the protonation site, but it is like that the calculation cannot reproduce these proximity effects adequately.

### Experimental

**Synthesis** Compounds **1** and **2** were synthesized as previously described.<sup>3,8)</sup> Free base **1**: mp 69 °C; oxalate **1**: mp 188 °C; free base **2**: mp 75–78 °C; oxalate **2**: mp 182 °C. *Anal.* (oxalate **2**) Calcd for C<sub>25</sub>H<sub>30</sub>N<sub>4</sub>O·C<sub>2</sub>H<sub>2</sub>O<sub>4</sub>: C, 65.84; H, 6.55; N, 11.37. Found C, 65.59; H, 6.55; N, 11.26.

**<sup>1</sup>H- and <sup>13</sup>C-NMR Spectroscopy** The NMR study was carried out with a Varian Unity 500 spectrometer operated at 499.9 MHz (<sup>1</sup>H), 125.7 MHz (<sup>13</sup>C). For <sup>1</sup>H and <sup>13</sup>C nuclei an inverse H–X detection probe equipped with gradients was used.

**X-Ray Crystallography** A colorless crystal of monohydrate hydrochloride salt with 0.33×0.33×0.50 mm was selected for the X-ray analysis. Selected structural details are listed in Table 4. The structure was solved by direct methods (Sir97)<sup>51)</sup> and the refinement process<sup>52)</sup> was carried out on Fo. All hydrogen atoms were located on difference Fourier maps and most were refined isotropically. The final atomic coordinates, thermal displacement pa-

Table 4. Crystal Data and Structure Refinement Parameters for Monohydrate Hydrochloride of **2**<sup>a)</sup>

Formula	C <sub>25</sub> H <sub>31</sub> N <sub>4</sub> O <sup>+</sup> ·Cl <sup>-</sup> ·H <sub>2</sub> O
Formula weight	457.02
Crystal system	Triclinic
Space group	P-1
a/Å	17.0224 (15)
b/Å	9.7519 (14)
c/Å	8.7306 (11)
α/°	119.082 (11)
β/°	95.401 (18)
γ/°	93.643 (15)
Z	2
T/K	295
Dc/g cm <sup>-3</sup>	1.213
μ/mm <sup>-1</sup>	1.568
Independent reflections	4093
Observed reflections (I > 2σ(I))	3124
R	0.043
wR	0.050

a) Full crystallographic data (CCDC 197014).

rameters, and geometric details were deposited with the Cambridge Crystallographic Data Centre (CCDC 197014).

**Theoretical Calculations** The structure of the neutral and protonated forms of fentanyl have been fully optimized with the B3LYP method and the 6-31G\* basis set using as a starting point the geometry found in X-ray crystallography. No significant changes were found between the X-ray structure and the calculated one. The theoretical NMR shieldings have been calculated using the GIAO<sup>43,44)</sup> method at the same level used for the geometry optimization.

**Acknowledgements** This work was supported by Grants BQU-2000-0868, BQU-2000-0906, and SAF-00-114-C02-01 from the Spanish DGI-CYT.

**Supporting Information Available** X-Ray crystallographic data for the structure of monohydrate hydrochloride salt of **2** has been deposited with the Cambridge Crystallographic Data Center under code CCDC 197014.

### References

- Jin W. Q., Paterson S. J., Kosterlitz H. W., Casy A. F., *Life Sci.*, **33**, 251–253 (1983).
- Bagley J. R., Kudzma L. V., Lalinde N. L., Colapret J. A., Huang B.-S., Lin B.-S., Jerussi T. P., Benvenega M. J., Doorley B. M., Ossipov M. H., Spaulding T. C., Spencer H. K., Rudo F. G., Wynn R. L., *Med. Res. Rev.*, **11**, 403–436 (1991).
- Janssen P. A. J., *Br. J. Anaesth.*, **34**, 260–268 (1962).
- Jeal W., Benfield P., *Drugs*, **53**, 109–138 (1997).
- Kanikkannan N., Kandimalla K., Lamba S. S., Singh M., *Curr. Med. Chem.*, **7**, 593–608 (2000).
- Cerezo L., Marin A., Zapatero A., Martín de Vidales C., López M., Perez-Torruja A., *Rev. Oncol.*, **2**, 159–163 (2000).
- Allan L., Hays H., Jensen N.-H., Le Polain de Waroux B., Bolt M., Donald R., Kalso E., *BMJ*, **322**, 1154–1158 (2001).
- Jagerovic N., Cano C., Elguero J., Goya P., Callado L. F., Meana J. J., Girón R., Abalo R., Ruiz D., Goicoechea C., Martín M. I., *Bioorg. Med. Chem.*, **10**, 817–827 (2002).
- Mićović I. V., Ivanovic M. D., Vuckovic S. M., Prostran M., Došen-Mićović L., Kiricojević V. D., *Bioorg. Med. Chem. Lett.*, **10**, 2011–2014 (2000).
- Chen B.-Y., Jin W.-Q., Chen J., Chen X.-J., Zhu Y.-C., Chi Z.-Q., *Life Sci.*, **65**, 1589–1595 (1999).
- Essawi M. Y. H., *Pharmazie*, **54**, 307–308 (1999).
- France C. P., Ahn S. C., Brockunier L. L., Bagley J. R., Brandt M. R., Winsauer P. J., Moerschbaecher J. M., *Pharm. Biochem. Behav.*, **59**, 295–303 (1998).
- Kudzma L. V., Evans S. M., Turnbull S. P., Jr., Severnak S. A., Ezell E. F., *Bioorg. Med. Chem. Lett.*, **5**, 1177–1182 (1995).
- Feldman P. L., James M. K., Brackeen M. F., Bilotta J. M., Schuster S. V., Lahe A. P., Lutz M. W., Johnson M. R., Leighton H. J., *J. Med. Chem.*, **34**, 2202–2208 (1991).
- Bagley O. R., Wynn R. L., Rudo F. G., Doorley B. M., Spencer H. K., *J. Med. Chem.*, **32**, 663–671 (1989).
- Llama E. F., Del Campo C., *J. Pharm. Pharmacol.*, **43**, 68–69 (1991).
- Cometta-Morini C., Loew G. H., *J. Comput.-Aided Mol. Design*, **5**, 335–356 (1991).
- Cometta-Morini C., Maguire P. A., Loew G. H., *Mol. Pharmacol.*, **41**, 185–196 (1992).
- Došen-Mićović L., Roglič G., Mićović I. V., Ivanović M., *Electron. J. Theor. Chem.*, **1**, 1999–210 (1996).
- Jiang H. L., Huang X. Q., Rong S. B., Luo X. M., Chen J. Z., Tang Y., Chen K. X., Zhu Y. C., Jin W. Q., Chi Z. Q., Ru Y. J., Cao Y., *Int. J. Quantum Chem.*, **78**, 285–293 (2000).
- Subramanian G., Ferguson D. M., *Drug Design Discovery*, **17**, 55–67 (2000).
- Filizola M., Villar H. O., Loew G. H., *J. Comp.-Aided Mol. Design*, **15**, 297–307 (2001).
- Martinez R., Rubio M. F., Alfaro L. J., Salcedo R., *J. Mol. Struct. (Theochem.)*, **342**, 141–146 (1995).
- Subramanian G., Paterlini G., Portoghese P. S., Ferguson D. M., *J. Med. Chem.*, **43**, 381–391 (2000).
- Allen F. H., Davies J. E., Galloy J. J., Johnson O., Kennard O., Macrae C. F., Mitchell E. M., Mitchell, J. F., Smith, J. F., Watson. D. G., *J. Chem. Info. Comput. Sci.*, **31**, 187–204 (1991).
- Duchamp D. J., Olson E. C., Chidester C. G., *Am. Crystallogr. Assoc.*,

- Ser. 2, **5**, 83—83 (1977).
- 27) Peeters O. M., Blaton N. M., De Ranter C. J., Van Herk A. M., Goubitz K., *J. Crystallog. Mol. Struct.*, **9**, 153—161 (1979).
- 28) Tollenaere J. P., Moereels H., Van Loon M., *Prog. Drug Res.*, **30**, 92—127 (1986).
- 29) Casey A. E., Hassan M. M. A., Simonds A. B., Stanniford D., *J. Pharm. Pharmacol.*, **21**, 434—440 (1969).
- 30) Brine G. A., Boldt K. G., Huang P.-T., Sawyer D. K., Caroll F. I., *J. Heterocycl. Chem.*, **26**, 677—685 (1989).
- 31) Karapetyan A. A., Struchkov Yu. T., Martirosyan V. O., Vartanyan R. S., Vartanyan S. A., *Zh. Strukt. Khim.*, **31**, 141—145 (1990).
- 32) Peeters O. M., Blaton N. M., De Ranter C. J., van Herk A. M., Goubitz K., *J. Cryst. Mol. Struct.*, **9**, 153—161 (1979).
- 33) Flippen-Anderson J. L., George C., Bertha C. M., Rice K. C., *Heterocycles*, **39**, 751—766 (1994).
- 34) Karapetyan A. A., Struchkov Yu. T., Martirosyan V. O., Vartanyan R. S., Vartanyan S. A., *Zh. Strukt. Khim.*, **30**, 185—189 (1989).
- 35) Karapetyan A. A., Struchkov Yu. T., Martirosyan V. O., Vartanyan R. S., Vartanyan S. A., *Zh. Strukt. Khim.*, **30**, 102—107 (1989).
- 36) Brine G. A., Stark P. A., Liu Y., Carroll F. I., Singh P., Xu H., Rothman R. B., *J. Med. Chem.*, **38**, 1547—1557 (1995).
- 37) Wang Z. X., Zhu Y. C., Ji R. Y., Lu Y., Tian Z. Y., Zheng Q. T., *Acta Pharm. Sin.*, **29**, 433—437 (1994).
- 38) Wang Z. X., Zhu Y. C., Jin W. Q., Chen X. J., Chen J., Ji R. Y., Chi Z. Q., *J. Med. Chem.*, **38**, 3652—3659 (1995).
- 39) Deschamps J. R., George C., Flippen-Anderson J. L., *Acta Crystallogr., Sect. C*, **58**, o362—o364 (2002).
- 40) Hariharan P. A., Pople J. A., *Theor. Chim. Acta*, **28**, 213—222 (1973).
- 41) Becke A. D., *J. Chem. Phys.*, **98**, 5648—5652 (1993).
- 42) Lee C., Yang W., Parr R. G., *Phys. Rev. B*, **37**, 785—789 (1998).
- 43) Ditchfield R., *Mol. Phys.*, **27**, 789—807 (1974).
- 44) London F., *J. Phys. Radium*, **8**, 397—409 (1937).
- 45) Faure R., Llinares J., Elguero J., *An. Quím.*, **81**, C, 167—172 (1985).
- 46) Etter M. C., *Acc. Chem. Res.*, **23**, 120—126 (1990).
- 47) Bernstein J., Davis R. R. E., Shimoni L., Chang N.-L., *Angew. Chem. Int. Ed. Engl.*, **34**, 1555—1573 (1995).
- 48) Pathaneni S. S., Desiraju G. R., *J. Chem. Soc. Dalton Trans.*, **1993**, 2505—2508 (1993).
- 49) Fernández-Castaño C., Foces-Foces C., Jagerovic N., Elguero J., *J. Mol. Struct.*, **355**, 265—271 (1995).
- 50) Steiner T., *Acta Crystallogr. Sect. B*, **54**, 456—463 (1998).
- 51) Altomare A., Burla M. C., Camalli M., Cascarano G., Giacovazzo C., Guagliardi A., Moliterni A. G. G., Polidori G., Spagna R., *J. Appl. Crystallogr.*, **32**, 115—119 (1999).
- 52) Hall S. R., du Boulay D. J., Olthof-Hazekamp O. (eds.), “The Xtal System of Crystallographic Software.” ‘Xtal3.6’ User’s Manual, University of Western Australia, Australia, 1999.